Optimal Day-ahead Operation Considering Power Quality for Active Distribution Networks

Yi Tan, *Member, IEEE*, Yijia Cao, *Senior Member, IEEE*, Yong Li, *Senior Member, IEEE*, Kwang Y. Lee, *Life Fellow, IEEE*, Lin Jiang, *Member, IEEE*, and Shuaihu Li

***Abstract*—Battery energy storage (BES) and distributed generation (DG) play an important role in active distribution networks. However, harmonic problems could be caused by the inverters in BES and DG, resulting in a poor power quality. In addition, ensuring acceptable voltage unbalance level is also another crucial power quality issue in distribution networks. Therefore, in this paper, an optimal distribution network operational model (ODNOM) is proposed to consider power quality problems caused by BES and DG. In this model, additional network power losses due to harmonics are considered into the objective function, and the harmonic constraints and voltage unbalance constraints are also taken into account. The particle swarm optimization (PSO) is used to solve the proposed ODNOM. Simulations on the IEEE 13-bus, IEEE 37-bus and IEEE 123-bus systems show that a satisfactory power quality can be achieved by the proposed approach while optimizing the total branch active power losses.**

***Note to Practitioners*—This paper aims to obtain a satisfactory power quality level while minimizing the total branch active power losses in the day-ahead dispatch of active distribution networks, since inverters-based BES and DG can inject harmonic pollution into distribution networks and voltage unbalance level is also an important issue for supplying good quality electricity to end users. To achieve such an objective, power quality constraints such as the total voltage harmonic distortion (THD) constraints, the individual voltage distortion constraints, and the voltage unbalance factor constraints are considered into the day-ahead scheduling. In addition, the network active power losses of the concerned harmonic frequencies are also considered into the objective function. The simulation results of the unbalanced IEEE 13-bus, IEEE 37-bus and IEEE 123-bus systems show that the proposed approach can give a satisfactory day-ahead schedule of good quality power for active distribution networks. Also, case studies indicate that total network power losses and the satisfactory power quality are the two contradictory objectives. The proposed approach can be applied to ensure a satisfactory power quality when making a dispatch plan in distribution networks with inverter-based BES and DG.**

***Index Terms*-- Active distribution networks, battery energy storage, day-ahead operation, distributed generation, power quality.**

This work was supported in part by the National Key Research and Development Program of China under Grant 2016YFB0900103, in part by the National Natural Science Foundation of China (NSFC) under Grant 61233008, and 51520105011, in part by the Key S&T Special Project of Hunan Province of China under Grant 2015GK1002, in part by the Fundamental Research Funds for the Central Universities of China (title: Distribution networks day-ahead dispatch method considering power quality); in part by the science and technology project of State Grid Corporation of China (title: Research and application of key technologies in smart grid park energy management and optimization for smart city). (*Corresponding author: Y. Li and Y. Cao*)

Y. Tan, Y. Cao and Y. Li are with the College of Electrical and Information Engineering, Hunan University, Changsha 410082, China (emails: yibirthday@126.com; yjcao@hnu.edu.cn; yongli@hnu.edu.cn).

K. Y. Lee is with the Department of Electrical and Computer Engineering, Baylor University, Waco, Texas 76798-7356, U.S.A. (email: Kwang_Y_Lee@baylor.edu).

L. Jiang and S. Li are with the Department of Electrical Engineering and Electronics, University of Liverpool, Liverpool L69 3GJ, U.K. (e-mail: L.Jiang@liverpool.ac.uk; shuaihu.Li@liverpool.ac.uk).

I. Introduction

As important components of smart grids, distributed generation (DG) and energy storage (ES) have received increasing attention in many countries. It is expected by Navigant that the installed capacity of DG will be larger than 165 GW in 2023, compared to 87.3 GW in 2014 [1]. Also, the advanced ES market in China will reach $8.7 billion and 31 GWh by 2025, which is three times bigger than the 2015 market [2].

Distributed generation and energy storage can bring many benefits to power systems. For example, power loss reduction [3] and investment deferral [4] can be achieved by DGs, and energy storage can help to integrate renewable DGs such as wind generator into power systems [5]. However, adverse effects can be also caused, including harmonic pollution because many DGs and ESs are integrated into distribution networks by inverters. In [6] and [7], it has been shown that distributed generation could cause the violation of total voltage harmonic distortion (THD) limit.

The harmonic regulation requirement has an important influence on distribution network operation and planning because:

1) Generally speaking, harmonic injection is positively related to the base-frequency power of harmonic resources. Large base-frequency output means large harmonic injection of harmonic resources. Therefore, the outputs of the inverter-based DG and ES with bad harmonic spectrum will be limited when the harmonic constraints are approaching to their limits.
2) With reference to [8], small harmonics injection may be amplified due to the resonance between capacitors and inductive elements in distribution networks when capacitors are not properly scheduled. That means it will cause severe power quality problem even though the harmonic injections of ES and DG are small.

Thus, it is necessary to consider harmonic pollution of DGs in distribution network operation and planning. Up until now, the harmonic constraints have been taken into account in optimal siting and sizing of DGs [9], the optimal integrated location and sizing of inverter based DGs and capacitors [10],

the determination of maximum penetration level of inverter based DG [11], assessing DG hosting capacity of distribution networks [12], and reactive power control with wind power [13].

In the field of distribution network operation, research has been carried out to consider DG and ES in [14]-[18], which are based on centralized optimization. It is known that a suitable information communications technology (ICT) is needed for the centralized optimization of active distribution networks. Centralized management is promising for active distribution networks if the ICT is improved to deal with large amount of information [19]. Furthermore, the centralized control structure has been also adopted in voltage control in the EU demonstration project of active distribution networks [20]. Therefore, it is feasible to adopt a centralized optimization based approach for day-ahead dispatch of distribution system with power quality considerations.

Voltage unbalance level is another important power quality (PQ) index for distribution networks. Voltage unbalance could cause negative effects, such as more losses [21]. Therefore, acceptable voltage unbalance level is required to supply good electricity to end-users, and it is important to limit the voltage unbalance level in distribution network operation.

To sum up, it is very desirable to consider power quality issues in distribution network operation. Therefore, in this paper, an optimal distribution network operational model (ODNOM) considering both harmonics and voltage unbalance is proposed for day-ahead dispatch of active distribution networks. In this model, the power quality constraints such as the total voltage harmonic distortion constraints, the individual voltage distortion constraints, and the voltage unbalance factor constraints are taken into consideration. Thus, the proposed approach can guarantee a satisfactory power quality in distribution network operation. In addition, a comprehensive objective function is formulated by incorporating the additional network active power losses due to harmonics for the whole dispatching period in the proposed ODNOM.

The rest of paper is organized as follows: The proposed ODNOM considering power quality is formulated in Section II. In Section III, the solution methodology is introduced to solve the proposed power quality based operational problem, and the simulation results of three unbalanced IEEE test systems are analyzed in Section IV. Finally, the conclusions are drawn for the proposed ODNOM and the simulation results in Section V.

II. Optimal Distribution Network Operational Model Considering Power Quality

In this section, the ODNOM is formulated to optimize network power losses while ensuring satisfactory power quality for active distribution networks as follows:

A. Objective Function

When the harmonic issue is considered, the corresponding network active power losses also need to be taken into account to give a comprehensive assessment on system economy [8]. Therefore, the network power losses of all concerned frequencies are considered into the objective function as follows:

$$F = \sum_{t=1}^{T}\left(P_{loss}^{t} + \sum_{h\in\Omega} P_{loss}^{t,h} \right) \tag{1}$$

where P_{loss}^{t} are the network active power losses of the base frequency at hour t and $P_{loss}^{t,h}$ are the network active power losses of the harmonic frequency h at hour t. Ω is the set of the concerned harmonic frequencies. Note that it is to optimize network active power losses in the proposed model, rather than energy losses, since a time interval of one hour is used for each sub-dispatching period. This has no influence on the optimal dispatch plan.

B. Power Quality Constraints

1) Total Harmonic Distortion Constraints:

In this paper, the total harmonic distortion (THD) is used to reflect the total harmonic level at bus i. Referring to [8], the following constraint is used:

$$\frac{\sum_{h\in\Omega}\left(V_{i,h}^{p,t}\right)^2}{V_{i}^{p,t}} \le THD_{i,\max}, \quad p = a,\ b,\ c \tag{2}$$

where $V_{i}^{p,t}$ and $V_{i,h}^{p,t}$ are respectively the voltage of base frequency and h-th harmonic frequency at the phase p of bus i at hour t, and $THD_{i,\max}$ is the upper limit of the total voltage harmonic distortion.

2) Individual Harmonic Distortion Constraints:

The individual harmonic distortion (IHD) is an index for assessing the harmonic level of each concerned frequency. With reference to [11], the IHD at bus i is constrained by:

$$\frac{V_{i,h}^{p,t}}{V_{i}^{p,t}} \le IHD_{i,\max}^{h} \tag{3}$$

where $IHD_{i,\max}^{h}$ is the upper limit of the individual voltage harmonic distortion of h-th harmonic frequency.

3) Voltage Unbalance Factor Constraints:

The voltage unbalance factor (VUF) can be used to reflect the unbalance level [21]-[22], and thus the following constraint is used to ensure a good voltage unbalance level:

$$\frac{V_{i}^{2,t}}{V_{i}^{1,t}} \times 100 \le UM\,\% \tag{4}$$

where $V_{i}^{1,t}$ and $V_{i}^{2,t}$ are the positive sequence and negative sequence voltages at bus i at hour t, respectively, and $UM\,\%$ is the limit of voltage unbalance factor in percentage. Note that only the voltages of base frequency are used to calculate the *VUF* as this index is defined for *sinusoidal* waves.

C. System Security Constraints

1) RMS Voltage Constraints:

$$V_{i,\min}^{p} \le V_{i,rms}^{p,t} \le V_{i,\max}^{p},\ p = a, b, c \tag{5}$$

where $$V_{i,rms}^{p,t} = \sqrt{\left(V_i^{p,t}\right)^2 + \sum_{h\in\Omega}\left(V_{i,h}^{p,t}\right)^2}$$

In (5), $V_{i,rms}^{p,t}$ is the *rms* voltage of the phase *p* at bus *i* at hour *t*. $V_{i,\min}^{p}$ and $V_{i,\max}^{p}$ are the lower and upper limits of $V_{i,rms}^{p,t}$, respectively.

2) RMS Current Constraints:

$$I_{ij,\min}^{p} \le I_{ij,rms}^{p,t} \le I_{ij,\max}^{p},\ p = a, b, c \tag{6}$$

where $I_{ij,rms}^{p,t}$ is the *rms* current of the phase *p* at the branch between bus *i* and bus *j* at hour *t*. $I_{ij,\min}^{p}$ and $I_{ij,\max}^{p}$ are the lower and upper limits of $I_{ij,rms}^{p,t}$, respectively. The $I_{ij,rms}^{p,t}$ are calculated as follows:

$$I_{ij,rms}^{p,t} = \sqrt{\left(I_{ij}^{p,t}\right)^2 + \sum_{h\in\Omega}\left(I_{ij,h}^{p,t}\right)^2} \tag{7}$$

where $I_{ij}^{p,t}$ and $I_{ij,h}^{p,t}$ are respectively the currents of base frequency and *h*-th harmonic frequency at the phase *p* of the branch between bus *i* and bus *j* at hour *t*. Note that this constraint is also applied to transformers in this paper.

D. Battery ES (BES) Constraints

With reference to [14], the battery energy storage is constrained with consideration of energy constraints, the power constraints and charge/discharge cycle constraint as follows:

1) Energy Constraints:

$$E_i^t = E_i^{t-1} - \varepsilon P_i^{ES,t}\Delta t \tag{8}$$

$$\varepsilon = \begin{cases} \varepsilon_{in} & P_i^{ES,t} < 0 \\ 1/\varepsilon_{out} & P_i^{ES,t} \ge 0 \end{cases} \tag{9}$$

$$E_i^{24} = E_i^0 \tag{10}$$

$$E_{i,\min} \le E_i^t \le E_{i,\max} \tag{11}$$

where E_i^t is the energy stored in BES *i* at the end of hour *t*, $E_{i,\max}$ and $E_{i,\min}$ are the upper and lower limits of E_i^t, respectively, $P_i^{ES,t}$ is the active power of BES *i* at hour *t*, and ε_{in} and ε_{out} are the charging and discharging efficiencies of BES, respectively.

In the above formulation, (8) presents the relationship between the energy level of two successive hours, (10) requires the final energy stored to be equal to the initial value, and the (11) limits the upper and lower bound of energy stored of BES *i*.

2) Power Constraints:

To ensure that the active power, reactive power and apparent power are within limits, they are constrained as follows:

$$-P_{i,\text{rated}}^{ES} \le P_i^{ES,t} \le P_{i,\text{rated}}^{ES} \tag{12}$$

$$Q_{i,\min}^{ES} \le Q_i^{ES,t} \le Q_{i,\max}^{ES} \tag{13}$$

$$\sqrt{\left(P_i^{ES,t}\right)^2 + \left(Q_i^{ES,t}\right)^2} \le S_{i,\max}^{ES} \tag{14}$$

where $P_{i,\text{rated}}^{ES}$ is the rated active power of BES *i*, $Q_{i,t}^{ES}$ is the reactive power of BES *i* at hour *t*, $Q_{i,\min}^{ES}$ and $Q_{i,\max}^{ES}$ are the lower and upper limits of $Q_{i,t}^{ES}$, respectively, and $S_{i,\max}^{ES}$ is the apparent power limit of BES *i*.

3) Charge/discharge Cycle Constraint

Due to the lifetime limits, it is suggested to allow only one charge/discharge cycle for BES in one day [14]. This is also adopted in this paper as follows:

$$N_i^{BES} \le 1 \tag{15}$$

where N_i^{BES} is the number of charge/discharge cycle of BES *i*.

E. Distributed Generator Constraints

$$P_{i,\min}^{DDG} \le P_i^{DDG,t} \le P_{i,\max}^{DDG} \tag{16}$$

$$\phi_{i,\min}^{DG} \le \phi_i^{DG,t} \le \phi_{i,\max}^{DG} \tag{17}$$

where $P_i^{DDG,t}$ is the active power of non-renewable distributed generator *i* at hour *t*, and $P_{i,\min}^{DDG}$ and $P_{i,\max}^{DDG}$ are the lower and upper limits of $P_i^{DDG,t}$, respectively. Using (16), the active power control of those distributed generators such as micro-turbines and fuel cells can be taken into account. $\phi_i^{DG,t}$ is the power factor angle of distributed generator *i* at hour *t*, and $\phi_{i,\min}^{DG}$ and $\phi_{i,\max}^{DDG}$ are the limits of $\phi_i^{DG,t}$. Using (17), the reactive power control of distributed generators can be considered [23].

F. Capacitor Constraints

$$Q_{i,\min}^{C,t} \le Q_i^{C,t} \le Q_{i,\max}^{C,t} \tag{18}$$

$$N_i^C \le N_{i,\max}^C \tag{19}$$

where $Q_i^{C,t}$ is the capacity of capacitors that are switched on at bus *i* at hour *t*, and $Q_{i,\min}^{C}$ and $Q_{i,\max}^{C}$ are its limits. Note that $Q_i^{C,t}$ is discrete decision variables in distribution network operation since the number of capacitors that are switched on is discrete. N_i^C is the number of switching actions and $N_{i,\max}^C$ is its limit. Equation (19) is to limit the number of switching actions to ensure good lifetime of capacitor bank.

G. Equality Constraints

The equality constraints are the power flow equations of base frequency and harmonic frequencies at each hour.

For the power flow of base frequency, it can be formulated using nodal current injection equations based on [24] as follows:

$$\begin{bmatrix} \boldsymbol{I}_1^{abc,t} \\ \vdots \\ \boldsymbol{I}_i^{abc,t} \\ \vdots \\ \boldsymbol{I}_n^{abc,t} \end{bmatrix} = \begin{bmatrix} \boldsymbol{y}_{11}^{abc,t} & \cdots & \boldsymbol{y}_{1j}^{abc,t} & \cdots & \boldsymbol{y}_{1n}^{abc,t} \\ \vdots & \ddots & \vdots & \iddots & \vdots \\ \boldsymbol{y}_{i1}^{abc,t} & \cdots & \boldsymbol{y}_{ij}^{abc,t} & \cdots & \boldsymbol{y}_{in}^{abc,t} \\ \vdots & \iddots & \vdots & \ddots & \vdots \\ \boldsymbol{y}_{n1}^{abc,t} & \cdots & \boldsymbol{y}_{nj}^{abc,t} & \cdots & \boldsymbol{y}_{nn}^{abc,t} \end{bmatrix} \begin{bmatrix} \boldsymbol{V}_1^{abc,t} \\ \vdots \\ \boldsymbol{V}_i^{abc,t} \\ \vdots \\ \boldsymbol{V}_n^{abc,t} \end{bmatrix} \tag{20}$$

where $\boldsymbol{I}_i^{abc,t} = \begin{bmatrix} I_i^{a,t} & I_i^{b,t} & I_i^{c,t} \end{bmatrix}^T$

$\boldsymbol{V}_i^{abc,t} = \begin{bmatrix} V_i^{a,t} & V_i^{b,t} & V_i^{c,t} \end{bmatrix}^T$

In the above formulation, $\boldsymbol{y}_{ij}^{abc,t}$ is sub-matrix of the node admittance matrix of base frequency at hour *t*; $\boldsymbol{I}_i^{abc,t}$ and $\boldsymbol{V}_i^{abc,t}$ are node current injection and voltage vectors of the base frequency at bus *i* at hour *t*, respectively. The node current injection can be from the load, DGs and BES, and $I_i^{a,t}$, $I_i^{b,t}$ and $I_i^{c,t}$ are the node current injections of phase-A, B and C of the base frequency at bus *i* at hour *t*, respectively. Finally, $V_i^{a,t}$, $V_i^{b,t}$ and $V_i^{c,t}$ are the voltages of phase-A, B and C of the base frequency at bus *i* at hour *t*, respectively.

Similarly, the power flow of the *h*-th harmonic frequency can be formulated based on [9], [25] and OpenDSS as follows:

$$\boldsymbol{I}_h^t = \boldsymbol{Y}_h^t \boldsymbol{V}_h^t \tag{21}$$

where

$\boldsymbol{I}_h^t = \begin{bmatrix} I_{1,h}^{a,t} & I_{1,h}^{b,t} & I_{1,h}^{c,t} \cdots & I_{i,h}^{a,t} & I_{i,h}^{b,t} & I_{i,h}^{c,t} & \cdots I_{n,h}^{a,t} & I_{n,h}^{b,t} & I_{n,h}^{c,t} \end{bmatrix}$

$\boldsymbol{V}_h^t = \begin{bmatrix} V_{1,h}^{a,t} & V_{1,h}^{b,t} & V_{1,h}^{c,t} \cdots & V_{i,h}^{a,t} & V_{i,h}^{b,t} & V_{i,h}^{c,t} & \cdots V_{n,h}^{a,t} & V_{n,h}^{b,t} & V_{n,h}^{c,t} \end{bmatrix}$

In above formulation, $I_{i,h}^{a,t}$, $I_{i,h}^{b,t}$ and $I_{i,h}^{c,t}$ are the node current injections of phase-A, B and C of the *h*-th harmonic frequency at bus *i* at hour *t*, respectively, $V_{i,h}^{a,t}$, $V_{i,h}^{b,t}$ and $V_{i,h}^{c,t}$ are the voltages of phase-A, B and C of the *h*-th harmonic frequency at bus *i* at hour *t*, respectively, and $\boldsymbol{Y}_h^t$ is node admittance matrix of the *h*-th harmonic frequency at hour *t*. The harmonic components of DGs and BES are modeled as a current source with one or more shunt branches. For the detailed model, interested authors are redirected to OpenDSS, which is used to solve the power flow problems of all concerned frequencies. The information about OpenDSS can be found in [26].

III. Solution Methodology

As the proposed ODNOM is to solve an optimization problem, the particle swarm optimization (PSO) is used as the optimizer in this paper.

A. Particle Swarm Optimization

Particle swarm optimization (PSO) is an effective heuristic optimization algorithm inspired by bird flocking [27] and it has received wide application in power system optimization such as economic dispatch [28]-[30], dynamic security control [31] and optimal power flow considering DG [32]. Since PSO is easy to implement and converges fast [33], it is employed to solve the proposed optimization problem.

In PSO, there is a group of particles searching for the optimum. To model animals' search behavior in optimization, the position and velocity are used as the attributes of each particle. For an optimization problem, a solution candidate can be represented by the position of a particle. At each iteration, each particle searches in the optimization space based on its last velocity, its individual historical best position, the global best position and its last position as follows [29], [33]:

$$V_{ij}^{k+1} = w_i^k V_{ij}^k + r_1 c_1 \left(X_{ij}^k - L_{ij}^k \right) + r_2 c_2 \left(X_{ij}^k - G_{ij}^k \right) \tag{22}$$

$$X_{ij}^{k+1} = X_{ij}^k + V_{ij}^{k+1} \tag{23}$$

where X_{ij}^k and V_{ij}^k are the *j*-th components of the position and the velocity of the *i*-th particle at iteration *k*, respectively. L_{ij}^k and G_{ij}^k are the *j*-th components of the individual historical best position and global best position, respectively. Parameters c_1 and c_2 are the weighting coefficients, r_1 and r_2 are the random numbers between 0 and 1, and w_i^k is the inertial coefficient at the *k*-th iteration. Inertial coefficient is generally decreased linearly as iteration number is increased [28].

B. Dealing with Constraints

When using the PSO to solve the proposed problem, the constraints must be dealt with. In this paper, constraints (2)-(6) are handled with the penalty function method used in [34]. For capacitor bank, its state will be set to the previous one if constraint (19) is violated.

The BES constraints are much more complex due to its temporal property. In this paper, an integrated penalty method and heuristic method is used to deal with the BES constraints. At hour *t*, the active and reactive powers of BES are modified to satisfy the constraints as follows:

Step 1) Check whether the number of charge/discharge cycles has reached its limit in previous period. If not, go to *Step 2)*; otherwise go to *Step 4)*;

Step 2) Calculate the current active power limit for BES considering (11) and (12). If the active power of BES violates this limit, then modify it to be the limit.

Step 3) Then check whether the number of charge/discharge cycles reach its limit. If not, go to *Step 5)* directly; otherwise, the state of BES cannot be changed anymore and the BES should be adjusted at this time as the energy stored in BES at *t*=24 cannot be more (less) than the initial value according to (10). In this case, the active power is modified as follows:

if $P_i^{ES,t} < 0$ and $E_i^t = E_i^{t-1} - \varepsilon_{in} P_i^{ES,t} \Delta t > E_i^0$

if $E_i^{t-1} > E_i^0$

$$P_i^{ES,t} = r_3 \bullet \min\left(P_{Dis\max}^{ES},\ P_{i,\text{rated}}^{ES} \right) \tag{24}$$

else

$$P_i^{ES,t} = r_4 \bullet \max\left(P_{\text{Cha}\max}^{ES},\ -P_{i,\text{rated}}^{ES} \right) \tag{25}$$

end

else if $P_i^{ES,t} > 0$ and $E_i^t = E_i^{t-1} - P_i^{ES,t}\Delta t / \varepsilon_{out} < E_i^0$

if $E_i^{t-1} > E_i^0$

$$P_i^{ES,t} = r_5 \bullet \min\left(P_{Dis\max}^{ES},\ P_{i,\text{rated}}^{ES}\right) \quad (26)$$

else

$$P_i^{ES,t} = r_6 \bullet \max\left(P_{\text{Cha}\max}^{ES},\ -P_{i,\text{rated}}^{ES}\right) \quad (27)$$

end

end

In (24)-(27), r_3, r_4, r_5, and r_6 are random numbers between 0 and 1, and $P_{Dis\max}^{ES}$ and $P_{\text{Cha}\max}^{ES}$ are defined as follows:

$$\begin{cases} P_{Dis\max}^{ES} = \left(E_i^{t-1} - E_i^0\right)\varepsilon_{out} / \Delta t \\ P_{\text{Cha}\max}^{ES} = \left(E_i^{t-1} - E_i^0\right) / \left(\varepsilon_{in}\Delta t\right) \end{cases}$$

After the modification, go to *Step 5)*;

Step 4) Modify the state of BES to be the previous state while keeping the absolute value of active power unchanged. In this case, the initial energy stored will be a boundary of energy stored because the (10) must be met at t=24. Therefore, the BES cannot be charged/discharged due to this constraint. Then the following modification will be done:

if $P_i^{ES,t} < 0$

if $P_i^{ES,t} < \left(E_i^{t-1} - E_i^0\right) / \left(\varepsilon_{in}\Delta t\right)$

if $t = 24$

$$P_i^{ES,t} = P_{\text{Cha}\max}^{ES} \quad (28)$$

else

$$P_i^{ES,t} = r_7 \bullet P_{\text{Cha}\max}^{ES} \quad (29)$$

end

end

else if $P_i^{ES,t} > 0$

if $P_i^{ES,t} > \varepsilon_{out}\left(E_i^{t-1} - E_i^0\right) / \Delta t$

if $t = 24$

$$P_i^{ES,t} = P_{Dis\max}^{ES} \quad (30)$$

else

$$P_i^{ES,t} = r_8 P_{Dis\max}^{ES} \quad (31)$$

end

end

else

$$P_i^{ES,t} = 0$$

end

In (29) and (31), r_7 and r_8 are random numbers between 0 and 1.

Step 5) If t=24, then judge whether $E_i^t \neq E_i^0$ or not. If so, penalize the fitness function.

Step 6) Calculate the current reactive power limit for BES considering (13) and (14). If this limit is violated, then set the reactive power of the BES to this limit.

Step 7) End the adjustment.

C. Solution Flowchart

As shown in Fig. 1, based on the PSO algorithm, the proposed ODNOM is solved as follows:

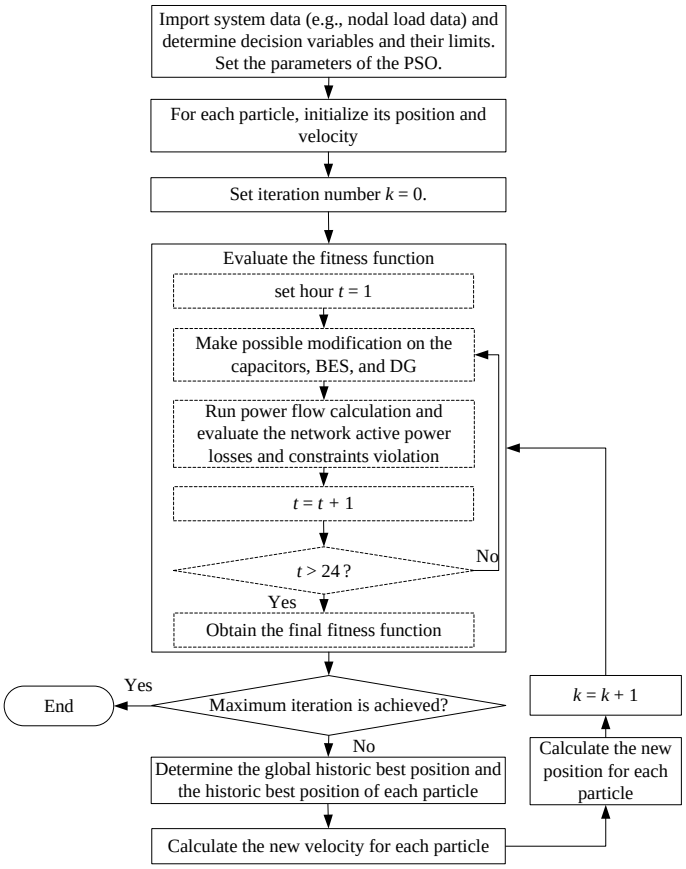

Fig. 1. Flow chart of solving ODNOM.

Step 1) Import distribution system data (e.g., nodal load data and line parameters) and determine the decision variables and their limits. Set the parameters of the PSO algorithm.

Step 2) Initialize the positions within their limits randomly, and initialize the velocities of the particles by using the method in [29];

Step 3) Evaluate the fitness function for each particle. The evaluation is based on the base-frequency and harmonic power flow analysis which is performed by the OpenDSS software of version 7.6.5.13. Note that the results of power losses are in the unit of *Watt* in OpenDSS. The state of BES is set to the discharging mode in power flow calculations in this paper if $P_i^{ES,t} \geq 0$. At the beginning of running the power flow analysis, the capacity of capacitor banks that are switched on are rounded off based on [35] because of its discrete nature. The outputs of BES are adjusted based on the method in the previous section. If the power flows are not converged, then the fitness

function will be penalized.

Step 4) Calculate the velocity of each particle first and then update the position. If any element of the position violates a limit, then it will be set to the limit.

Step 5) Evaluate the fitness function for each particle by using the method in *Step 3)*.

Step 6) Update the individual historical best position for each particle and determine the global best position;

Step 7) If the maximum iterations are achieved, then end the optimization process; otherwise go to *Step 4)*.

IV. Case Study

In this section, the IEEE 13-bus, IEEE 37-bus, and IEEE 123-systems are used to validate the proposed approach. The detailed data can be found in the OpenDSS software. For each system, the hourly active power of total load and wind generation (WG) is assumed based on [36] and [37], respectively. Note that the power factor of bus load remains unchanged when the active power is modified based on [36] and the default load in OpenDSS. In the three systems, the current limits of each phase of distribution lines are set to 600A and the rated currents of three-phase transformers are increased to be $\sqrt{3}$ times of the original values. The WG and fuel cell (FC) are added and modeled by the Generator Object of OpenDSS, and the harmonic spectrums of WG and FC are set based on [7]. The BES is also added and modeled by using Storage Object without a consideration of idling losses. The charging and discharging efficiencies are both set to 0.9, and the initial value, upper and lower limits of stored energy are assumed to be 50%, 90% and 20% of rated energy, respectively. The default harmonic spectrums of BES and harmonic Load in OpenDSS are used in this paper. Some of their parameters are given in Tables I-IV, and others are set to default values in OpenDSS. The capacitors are assumed to be switchable, and the maximum number of switching action is 5. The adjustable size of the capacitors are one fifth of their capacities.

In all the following simulation, the upper and lower voltage limits are set to 1.10 and 0.90 in per unit, respectively, and the total and individual voltage harmonic distortion limits are set to 5% and 3%, respectively [11]. Considering that, for the base frequency, the ratio between 95% of the 600-second mean rms value of the negative-phase-sequence voltage and the positive-phase-sequence one should be no more than 2% at a supply terminal at each period of one week in normal cases [38], this value is used as the limit of voltage unbalance factor in this paper. The approach without consideration of power quality, i.e., no power quality approach (NPQ), is used for comparison. The power losses due to harmonics are not considered in the NPQ approach. For each case, the best results of 30 runs are chosen for analysis since PSO is a stochastic algorithm [33].

A. IEEE 13-bus system

As shown in Fig. 2, the modified IEEE 13-bus system with BES, WG, and FC are studied in this section. In Fig. 2, voltage regulators, loads and capacitors are not shown. Note that voltage regulators are modelled as autotransformers in OpenDSS and thus the topology in Fig.2 is a little different from the one in OpenDSS. The network topology in OpenDSS is actually used in our simulations. In this study, two cases are considered with different sizes and siting of BES, as shown in Table I. Note that the BES is installed at 480V-side of the transformer in the Case 2 and it has a small capacity. In this system, there is a switch between bus 671 and bus 692. The switch is closed in our simulation. The hourly active wind power and load is shown in Fig. 3.

The simulation results are shown in Figs. 4-10 and Table V. Since both NPQ approach and the proposed approach gives no violation of IHD constraints in Case 1 and no violation of both IHD and THD constraints in Case 2, the corresponding results are not presented.

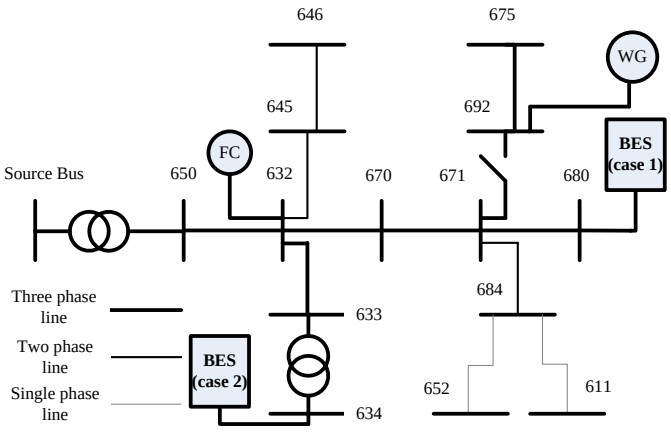

Fig. 2. The modified IEEE 13-bus system of Case 1 and Case 2.

TABLE I
THE PARAMETERS OF BES IN THE TEST SYSTEMS

		Bus	Rated power (kVA)	Rated active power (kW)	Maximum reactive power (kVar)	Rated stored energy (kWh)
IEEE 13-bus system	Case 1	680	100	100	100	800
	Case 2	634	10	10	10	40
IEEE 37-bus system		709	100	100	100	800
IEEE 123-bus system		78	100	100	100	800
		67	100	100	100	800

TABLE II
WIND POWER PARAMETERS IN THE TEST SYSTEMS

	Bus	Capacity (kW)	Power factor angle	
			Upper limit	Lower limit
IEEE 13-bus system (Case 1& Case 2)	692	300	arccos (0.9)	-arccos (0.9)
IEEE 37-bus system	731	200	arccos (0.9)	-arccos (0.9)
	735	200	arccos (0.9)	-arccos (0.9)
IEEE 123-bus system	81	200	arccos (0.9)	-arccos (0.9)
	67	200	arccos (0.9)	-arccos (0.9)

TABLE III
THE PARAMETERS OF FC IN THE TEST SYSTEMS

	Bus	Active power (kW)		Power factor angle	
		Upper limit	Lower limit	Upper limit	Lower limit
IEEE 13-bus system (Case 1& Case 2)	632	300	0	arccos (0.9)	-arccos (0.9)
IEEE 37-bus system	744	400	0	arccos (0.9)	-arccos (0.9)
IEEE 123-bus system	98	300	0	arccos (0.9)	-arccos (0.9)

TABLE IV
THE HARMONIC LOADS IN THE TEST SYSTEMS

	IEEE 13-bus system		IEEE 37-bus system	IEEE 123-bus system
	Case 1	Case 2		
Harmonic load bus and phase	bus 675 (B-phase) bus 634 (C-phase)	bus 670 bus 652 (A-phase)	bus 742 (B-phase) bus 722 (C-phase) bus 714 (A-phase) bus 738	bus 76 bus 65

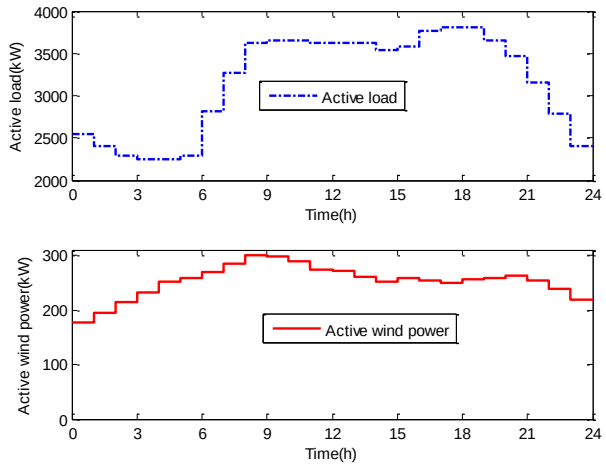

Fig. 3. The active power of total load and wind power generation.

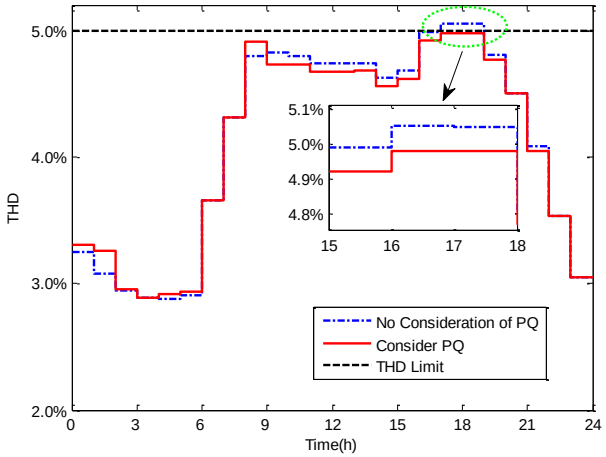

Fig. 4. The maximum THD for each hour in the IEEE 13-bus system (Case 1).

From Fig. 4-6, one can conclude that there are no violations of THD and VUF constraints in Case 1 and Case 2 if the proposed approach is used. In contrast, NPQ approach gives violations of THD and VUF constraints in Case 1 and the violations of VUF constraint in Case 2. Therefore, satisfactory power quality can be obtained by the proposed approach. As shown in Table V, the proposed approach gives higher total power losses. This is because more constraints such as THD constraints and VUF constraints are considered. From Table V, it should be noted that larger harmonic power losses and lower power losses of base frequency are obtained if power quality issue is not taken into account. That means harmonic power losses and the power losses of base frequency are contradictory objectives. The harmonic power losses are reduced because the harmonic issues are considered into the objective function. Also, note that the harmonic power losses are reduced by 35.32% in Case 2 while the power losses of base frequency are increased by 7.55%, although the decrease rate of the harmonic power losses is smaller than the increase rate of the power losses of base frequency in Case 1. Therefore, significant harmonic power losses can be reduced by the proposed approach in some cases.

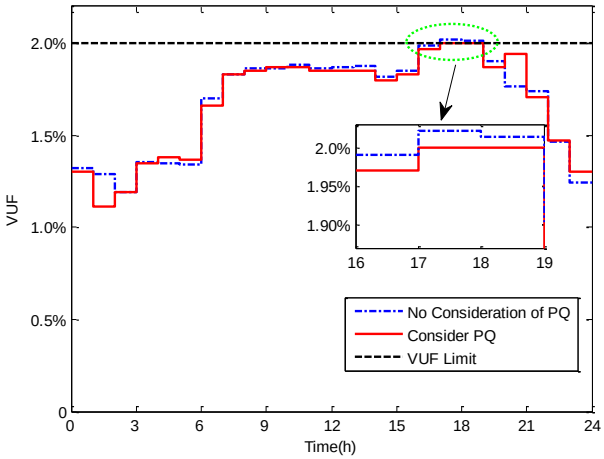

Fig. 5. The maximum VUF for each hour in the IEEE 13-bus system (Case 1).

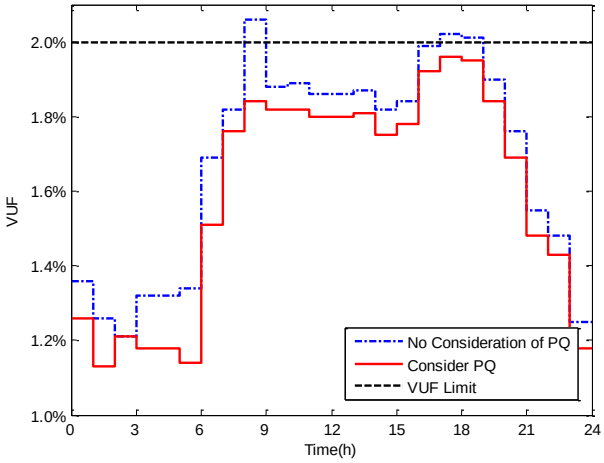

Fig. 6. The maximum VUF for each hour in the IEEE 13-bus system (case 2).

TABLE V
THE COMPARISON OF POWER LOSSES BETWEEN THE PROPOSED APPROACH AND NPQ APPROACH IN IEEE 13-BUS SYSTEM

		Power losses of base frequency (kW)	Power losses due to harmonics (kW)	Total power losses (kW)
Case 1	NPQ	1759.076	6.156	1765.232
	with PQ	1784.514	6.120	1790.634
Case 2	NPQ	1783.116	9.558	1792.673
	with PQ	1917.657	6.182	1923.839

Due to limited space, Figs. 7-10 only presented the outputs of BES and the capacities of capacitors that are switched on. From Figs. 7-8, one can observe that the outputs of BES will change significantly if power quality issue is considered. In Figs. 9-10, the capacities of capacitors that are switched on are very different at some dispatch periods in both Case1 and Case 2. From the above analysis, it can be concluded that the optimal schedule will be significantly changed if power quality issue is incorporated into day-ahead operation of distribution networks.

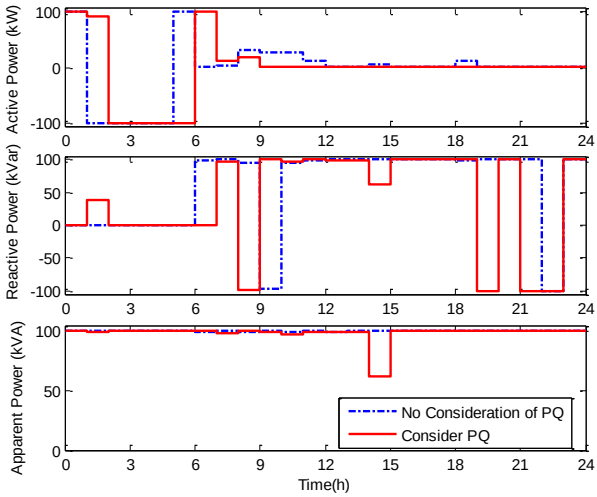

Fig. 7. The active, reactive and apparent power of BES in the IEEE 13-bus system (Case 1).

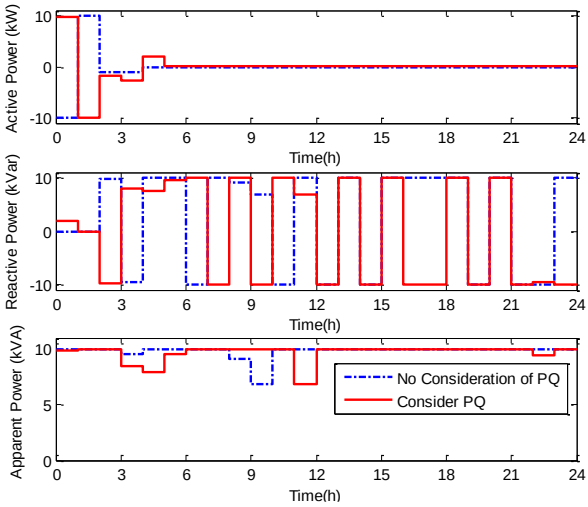

Fig. 8. The active, reactive and apparent power of BES in the IEEE 13-bus system (Case 2).

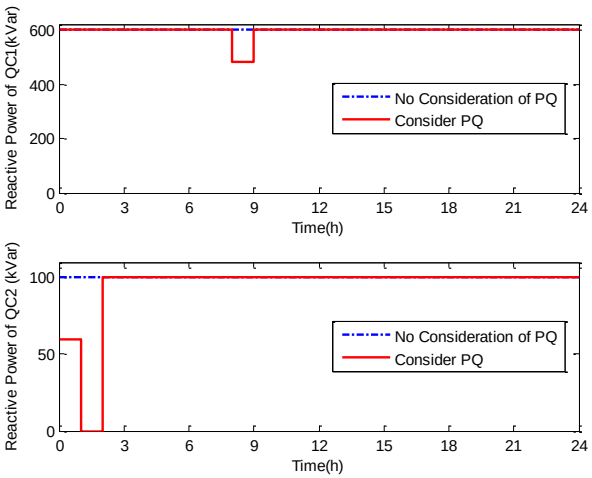

Fig. 9. The capacities of the capacitors that are switched on in the IEEE 13-bus system (Case 1).

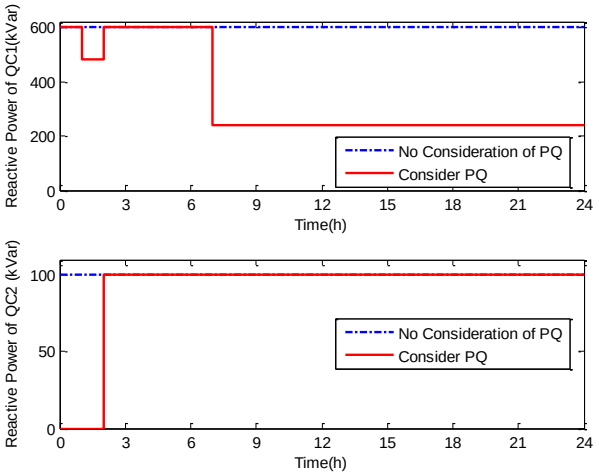

Fig. 10. The capacities of the capacitors that are switched on in the IEEE 13-bus system (Case 2).

B. IEEE 37-bus system and IEEE 123-bus system

In this section, the IEEE 37-bus system and the IEEE 123-bus system are further used to validate the feasibility of our approach in larger systems. In this case study, FC, WG and BES are added to the test systems, as shown in Tables I-III. For the IEEE 37-bus system, two capacitor banks of [0 400] kVar with a discrete step of 80 kVar are assumed to be installed at buses 737 and 706, respectively. The results are shown in Figs. 11-13 and Table VI.

As shown in Figs. 11-13, similar to the results of IEEE 13-bus system, the proposed approach also gives no violations of power quality constraints. In contrast, the IHD constraints are violated for nearly half a day in the IEEE 37-bus system and both the THD and IHD constraints are violated for more than half a day in the IEEE 123-bus system. That means a satisfactory harmonic level cannot be achieved. Therefore, our approach gives a much better power quality profile. As shown in Table VI, the power losses are further compared in both the IEEE 37-bus system and IEEE 123-bus system. Still, the proposed approach gives higher power losses of base frequency and lower harmonics power losses, as compared to the approach without consideration of power quality.

Moreover, a satisfactory power quality level is achieved at the cost of lowering economy. Also, note that the harmonic power losses are reduced by 41.81% and 66.24% in IEEE 37-bus and IEEE 123-bus systems, respectively, while the power losses of base frequency are only increased by 6.64% and 5.41%, respectively. Therefore, a harmonic power losses reduction rate are much higher than the increase rate of power losses of base frequency in both test systems.

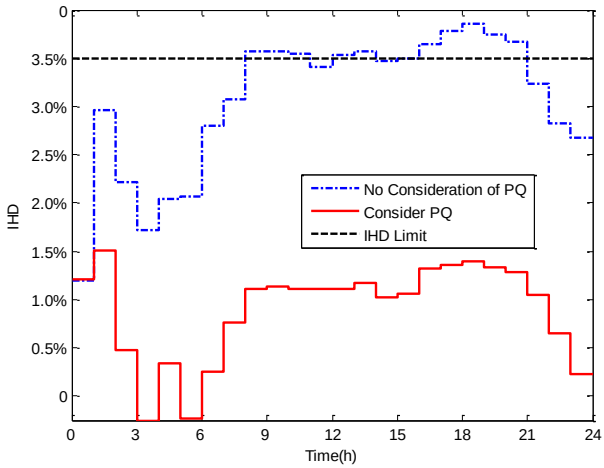

Fig. 11. The maximum IHD for each hour in the IEEE 37-bus system.

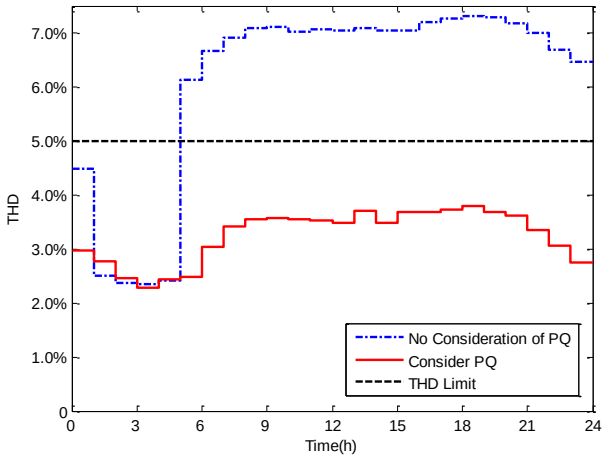

Fig. 12. The maximum THD for each hour in the IEEE 123-bus system.

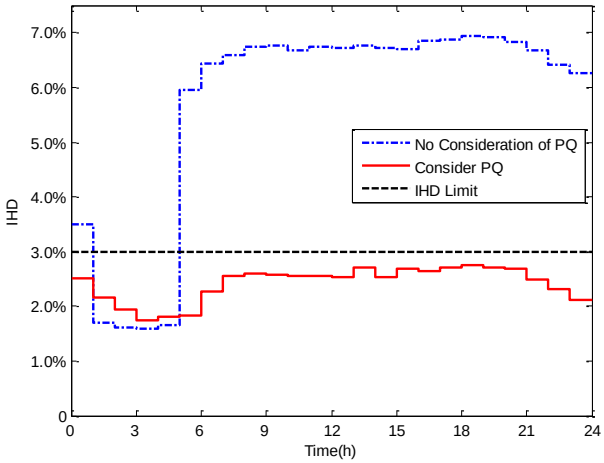

Fig. 13. The maximum IHD for each hour in the IEEE 123-bus system.

TABLE VI
THE COMPARISON OF POWER LOSSES BETWEEN THE PROPOSED APPROACH AND THE NPQ APPROACH IN IEEE 37-BUS AND IEEE 123-BUS SYSTEMS

		Power losses of base frequency (kW)	Power losses due to harmonics (kW)	Total power losses (kW)
IEEE 37 Bus system	NPQ	1275.835	9.559	1285.394
	with PQ	1360.537	5.562	1366.099
IEEE 123 Bus system	NPQ	1170.945	23.191	1194.137
	with PQ	1234.264	7.829	1242.092

C. Analysis on Computational Performance

In this section, the computational performance of the PSO based approach on solving the proposed problem is investigated. First, the convergence curves of the proposed PSO based approach of all previous cases are given in Figs. 14-17. From those figures, one can see that that the proposed approach has a good convergence in the three test systems.

Furthermore, the statistical analysis of the PSO based approach is investigated on solving the proposed problem in the IEEE 123-bus system. Four cases are studied and the results of each case are analyzed based on 30 runs. In Table VII, the minimum value, average value and standard deviation of the fitness function of the proposed optimization problem are studied. In this table, Case 3.4 represents the case of previous IEEE 123 bus system study and the load levels of Cases 3.1-3.3 are 70%, 80%, 90% of Case 3.4. From this table, it can be seen that the proposed approach is robust since the standard deviations are very small as compared to the average values and the difference between the minimum value and the average value are small in most of cases (see Cases 3.1-3.3). In addition, no infeasible solution is found in Cases 3.1-3.3. In contrast, in Case 3.4, very large average value is obtained since many infeasible solutions are found by the PSO-based approach. This is because the load level is heavy in Case 3.4 and the constraints are much more tight than other cases, leading to a hard optimization problem. However, the proposed approach can still obtain satisfactory solutions in 30 runs, which cause no violation of power quality constraints as shown in the previous section. Therefore, the proposed PSO

based approach performs well on solving the proposed day-ahead dispatch problem with consideration of power quality in distribution networks.

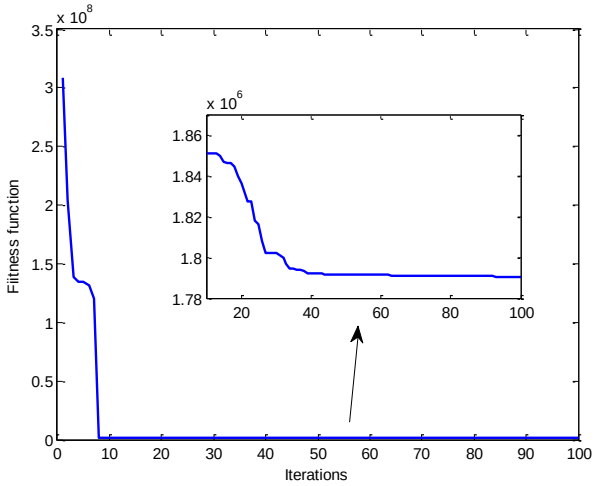

Fig. 14. Convergence of proposed approach in IEEE 13-bus system (Case 1).

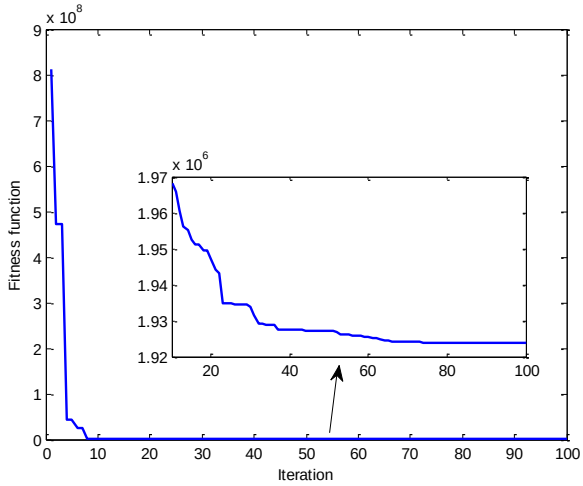

Fig. 15. Convergence of proposed approach in IEEE 13-bus system (Case 2).

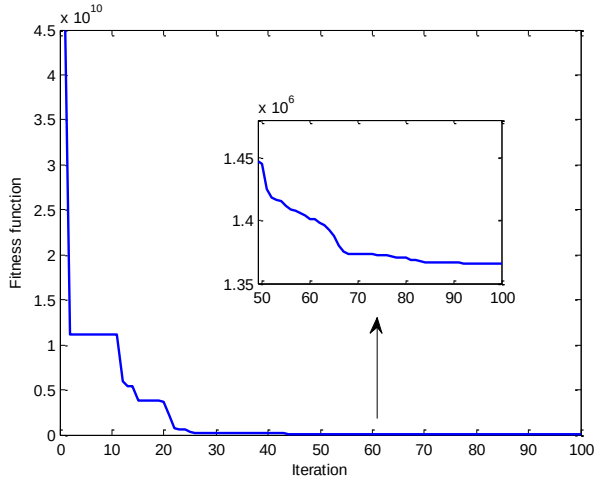

Fig. 16. Convergence of the proposed approach in the IEEE 37-bus system.

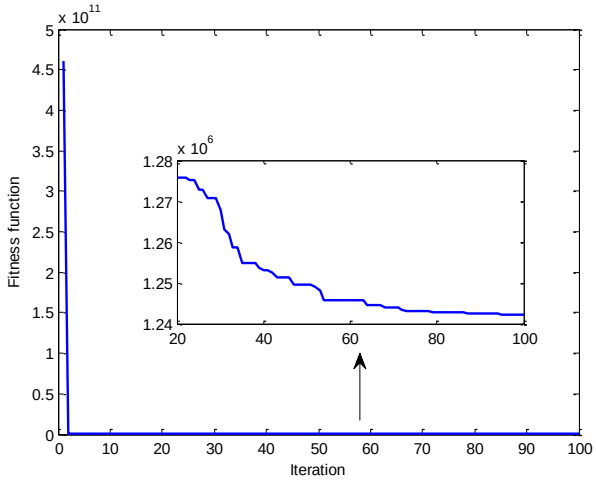

Fig. 17. Convergence of the proposed approach in the IEEE 123-bus system.

TABLE VII
THE STATISTICAL ANALYSIS OF THE PROPOSED APPROACH ON THE IEEE 123-BUS SYSTEM

	Fitness value		
	Minimum ($\times 10^3$)	Standard deviation ($\times 10^3$)	Average ($\times 10^3$)
Case 3.1 (η=70%)	489.653	12.422	507.673
Case 3.2 (η=80%)	691.562	27.326	732.182
Case 3.3 (η=90%)	934.949	31.788	1000.674
Case 3.4 (η=100%)	1242.092	74379561.389	271510302.210

η represents different load level. Each case is based on 30 independent runs.

D. Remarks

In this paper, the proposed optimization approach is based on the centralized control structure. If the distributed control structure is used, then the controllable units should make decision based on local information, e.g., voltage unbalance factor and the harmonic distortion at its connection point. Also neighbor's power quality information may be used depending on the distributed communication structure. In this case, coordination between controllable units should be made to achieve the optimal schedule under power quality constraints.

V. CONCLUSIONS AND FUTURE WORKS

In this paper, an optimal distribution network operational model is proposed to consider the power quality problem caused by DG and BES when making day-ahead dispatch plan. The harmonic constraints and voltage unbalance constraint are considered into the mathematical formulation. In addition, the harmonic power losses are included into the objective function to give a comprehensive optimization on operational economy. Thus, the harmonic pollution and voltage unbalance impacts due to distributed generation and battery energy storage can be comprehensively taken into account. Simulations show that a satisfactory power quality level can be achieved by the proposed approach with significant different solutions as compared to the no power quality approach. Thus, the proposed approach is promising in ensuring good-quality electricity-supply in active distribution network operation. In

addition, our simulation also indicates satisfactory power quality and good operational economy are contradictory. More total power losses are caused if the power quality constraints are required to be met. Wind power is uncertain in nature. However, this is not considered in this paper. In future research, we will focus on a stochastic operational model with consideration of both power quality and uncertainty.

VI. References

[1] J. S. Hill, "Distributed generation capacity expected to double by 2023," http://cleantechnica.com/2014/12/09/distributed-generation-capacity-expected-double-2023/

[2] M. Stone, "Advanced energy storage demand to quadruple in China in 10 years," https://www.greentechmedia.com/articles/read/advanced-energy-storage-demand-to-quadruple-in-china.

[3] M.-R. Haghifam, H. Falaghi, and O. Malik, "Risk-based distributed generation placement," *IET Gen., Transm., Distrib.*, vol. 2, no. 2, pp. 252–260, Mar. 2008.

[4] A. Piccolo and P. Siano, "Evaluating the impact of network investment deferral on distributed generation expansion," *IEEE Trans. Power Syst.*, vol. 24, no. 3, pp. 1559–1567, Aug. 2009.

[5] M. Y. Suberua, M. W. Mustafaa, and N. Bashir, "Energy storage systems for renewable energy power sector integration and mitigation of intermittency," *Renewable and Sustainable Energy Reviews*, vol. 35, pp. 499–514, Jul. 2014.

[6] A. F. A. Kadir, A. Mohamed, and H. Shareef, "Harmonic impact of different distributed generation units on low voltage distribution system," *2011 IEEE International Electric Machines & Drives Conference*.

[7] S. Abdelrahman, H. Liao, J. Yu, and J. V. Milanovic, "Probabilistic assessment of the impact of distributed generation and non-linear load on harmonic propagation in power networks," *2014 Power Systems Computation Conference*.

[8] A. A. Eajal and M. E. El-Hawary, "Optimal capacitor placement and sizing in unbalanced distribution systems with harmonics consideration using particle swarm optimization," *IEEE Trans. Power Delivery*, vol. 25, no. 3, pp. 1734–1741, Jul. 2010.

[9] S. Biswas, S. K. Goswami, and A. Chatterjee, "Optimal distributed generation placement in shunt capacitor compensated distribution systems considering voltage sag and harmonics distortions," *IET Gen., Transm., Distrib.*, vol. 8, no. 5, pp. 783 – 797, May 2014.

[10] N. Ghaffarzadeh and H. Sadeghi, "A new efficient BBO based method for simultaneous placement of inverter-based DG units and capacitors considering harmonic limits," *International Journal of Electrical Power and Energy Systems*, vol. 80, pp. 37 – 45, Sep. 2016.

[11] V. R. Pandi, H. H. Zeineldin, W. Xiao, and A. F. Zobaa, "Optimal penetration levels for inverter-based distributed generation considering harmonic limits," *Electric Power System Research*, vol. 97, pp. 68–75, Apr. 2013.

[12] S. Wei, G. P. Harrison, and S. Z. Djokic, "Distribution network capacity assessment: incorporating harmonic distortion limits," *2012 IEEE Power and Energy Society General Meeting*, pp. 1-7, 2012.

[13] S. Jashfar, M. M. Hosseini-Biyouki, and S. Esmaeili, "A stochastic programming to Volt/VAR/Total harmonic distortion control in distribution networks including wind turbines," *Electric Power Components and Systems*, vol. 43, no.7, pp.733–746, 2015

[14] A. Gabash and P. Li, "Active-reactive optimal power flow in distribution networks with embedded generation and battery storages," *IEEE Trans. Power Systems*, vol. 27, no. 4, pp. 2026- 2035, Nov. 2012.

[15] A. Gabash and P. Li, "Flexible optimal operation of battery storage systems for energy supply networks," *IEEE Trans. Power Systems*, vol. 28, no. 3, pp. 2788 - 2797, Aug. 2013.

[16] S. Gill, I. Kockar, and G. W. Ault, "Dynamic optimal power flow for active distribution networks," *IEEE Trans. Power Systems*, vol. 29, no. 1, pp. 121 - 131, Jan. 2014.

[17] L. H. Macedo, J. F. Franco, M. J. Rider, and R. Romero, "Optimal operation of distribution networks considering energy storage devices," *IEEE Trans. Smart Grid*, vol. 6, no. 6, pp. 2825-2836, Nov. 2015.

[18] A. Soroudi, P. Siano, and A. Keane, "Optimal DR and ESS scheduling for distribution losses payments minimization under electricity price Uncertainty," *IEEE Trans. Smart Grid*, vol. 7, no. 1, pp. 261-272, Jan. 2016.

[19] Specification of Active Distribution Network Concept. Deliverable 2.1, IDE4L EU Project. [Online]. Available: http://www.danskenergi.dk/AndreSider/Forskning/~/media/6D56160D54A8496B97FEB76035749FC2.ashx.

[20] Samuelsson, S. Repo, R. Jessler, J. Aho, M. Kärenlampi, and A. Malmquist, "Active distribution network – demonstration project ADINE," 2010 IEEE PES Innovative Smart Grid Technologies Conference Europe (ISGT Europe), 2010.

[21] A. Jouanne and B. Banerjee, "Assessment of voltage unbalance," *IEEE Trans. Power Del.*, vol. 16, no. 4, pp. 782–790, Oct. 2001.

[22] N. C. Woolley and J. V. Milanović, "Statistical estimation of the source and level of voltage unbalance in distribution networks," *IEEE Trans. Power Delivery*, vol. 27, no. 3, pp. 1450–1460, Jul. 2012.

[23] L. F. Ochoa, A. Keane, and G. P. Harrison, "Minimizing the reactive support for distributed generation: enhanced passive operation and smart distribution networks," *IEEE Trans. Power Systems*, vol. 26, no. 4, pp. 2134-2142, Nov. 2011.

[24] For "Newton" algorithm [Online]. Available: https://sourceforge.net/p/electricdss/discussion/861976/thread/54500bb5/?limit=25#419a. Accessed date: Jun. 2016.

[25] Y. Baghzouz, "Effects of nonlinear loads on optimal capacitors placement in radial feeders," *IEEE Transactions on Power Delivery*, vol. 6, no. 1, pp. 245-251, Jan. 1991

[26] *Simulation Tool – OpenDSS*. http://smartgrid.epri.com/SimulationTool.aspx.

[27] X. Chen, W. Du, H. Tianfield, R. Qi, W. He, and F. Qian, "Dynamic optimization of industrial processes with nonuniform discretization-based control vector parameterization," *IEEE Trans. Automation Science and Engineering*, vol. 11, no. 4, pp. 1289-1299, Oct. 2014.

[28] Z. Gaing, "Particle swarm optimization to solving the economic dispatch considering the generator constraints," *IEEE Trans. Power Systems*, vol. 18, no.3, pp.1187-1195, Aug. 2003.

[29] A. I. Selvakumar and K. Thanushkodi, "A new particle swarm optimization solution to nonconvex economic dispatch problems," *IEEE Trans. Power Syst.*, vol. 22, no.1, pp. 42-51, Feb. 2007.

[30] J.-B. Park, Y.-W. Jeong, J.-R. Shin, and K. Y. Lee, "An improved particle swarm optimization for nonconvex economic dispatch problems," *IEEE Trans. on Power Systems*, vol. 25, no. 1, pp. 156- 166, Feb. 2010.

[31] N. D. Hatziargyriou and E. M. Voumvoulakis, "A particle swarm optimization method for power system dynamic security control," *IEEE Trans. Power Systems*, vol. 25, no.2, pp. 1032 - 1041, May 2010.

[32] Q. Kang, M. Zhou, J. An, and Q. Wu, "Swarm intelligence approaches to optimal power flow problem with distributed generator failures in power networks," *IEEE Trans. Automation Science and Engineering*, vol. 10, no. 2, pp. 343-353, Apr. 2013.

[33] S. Song, L. Kong, Y. Gan, and R. Su, "Hybrid particle swarm cooperative optimization algorithm and its application to MBC in alumina production," *Progress in Natural Science*, vol. 18, no. 11, pp. 1423–1428, Nov. 2008.

[34] W. Yan, F. Liu, C. Y. Chung, and K. P Wong, "A hybrid genetic algorithm-interior point method for optimal reactive power flow," *IEEE Trans. Power Systems*, vol. 21, no. 3, pp. 1163–1169, Aug. 2006.

[35] M. R. AlRashidi and M. E. El-Hawary, "Hybrid particle swarm optimization approach for solving the discrete OPF problem considering the valve loading effects," *IEEE Trans. Power Systems*, pp.2030 – 2038, vol. 22, no.4, Nov. 2007.

[36] The IEEE Reliability Test System (IEEE-RTS). https://www.ee.washington.edu/research/pstca/rts/rts79/ieeerts79.txt

[37] Wind Power Production - Hourly averaged actual and forecasted values. http://mis.ercot.com/misapp/GetReports.do?reportTypeId=13028&reportTitle=Wind%20Power%20Production%20-%20Hourly%20Averaged%20Actual%20and%20Forecasted%20Values&showHTMLView=&mimicKey

[38] *Application Note - Standard EN 50160 / Voltage characteristics of electricity supplied by public electricity networks*, European Copper Institute, Mar. 2013